A thin drop sliding down an inclined plate

E. S. Benilov[1],† and M. S. Benilov[2,3]

[1]Department of Mathematics and Statistics, University of Limerick, Ireland

[2]Departamento de Física, CCCEE, Universidade da Madeira, Largo do Município,
9000 Funchal, Portugal

[3]Instituto de Plasmas e Fusão Nuclear, Instituto Superior Técnico, Universidade de Lisboa, Portugal

We examine two- and three-dimensional drops steadily sliding down an inclined
plate. The contact line of the drop is governed by a model based on the Navier-slip
boundary condition and a prescribed value for the contact angle. The drop is thin,
so the lubrication approximation can be used. In the three-dimensional case, we
also assume that the drop is sufficiently small (its size is smaller than the capillary
scale). These assumptions enable us to determine the shape of the drop and derive
an asymptotic expression for its velocity. For three-dimensional drops, this expression
is matched to a qualitative estimate of Kim *et al.* (*J. Colloid Interface Sci.*, vol. 247,
2002, pp. 372–380) obtained for arbitrary drops, i.e. not necessarily thin and small.
The matching fixes an undetermined coefficient in Kim, Lee and Kang's estimate,
turning it into a quantitative result.

Key words: drops, interfacial flows (free surface), thin films

1. Introduction

Given that several self-consistent, yet conflicting, models of contact lines (CLs)
exist, one can only judge them by comparing their predictions with the experimental
data. Such comparisons typically involve the predicted/measured values of the dynamic
contact angle (e.g. Le Grand, Daerr & Limat 2005; Rio *et al.* 2005).

It should be noted, however, that the dynamic contact angle and similar local
characteristics (with short-scale variability) are much harder to measure than global
parameters, such as, say, the velocity of a drop sliding down an inclined plate. Such
a setting, in fact, can be viewed as the simplest testbed for theoretical models of CLs,
and it indeed has been used as such by Kim, Lee & Kang (2002) and Puthenveettil,
Senthilkumar & Hopfinger (2013) to test a qualitative estimate derived in the former
paper. This estimate, however, involves an undetermined constant, hampering the
comparison with the experimental data and, thus, suggesting a need for a quantitative
theory for drops sliding down an incline.

The first such theory was obtained by Hocking (1981) for two-dimensional (2D)
thin drops described by the lubrication approximation. For the CLs he used the
Navier-slip boundary condition and the assumption that the contact angle of an

† Email address for correspondence: Eugene.Benilov@ul.ie

advancing (receding) CL equals θ_a (θ_r), whereas that of a static CL can assume any value between θ_r and θ_a. In particular, it was shown that sufficiently large drops develop a 'tail' of almost uniform thickness. Once the tail has emerged, further increases of the drop's mass cause only an increase in the length of the tail, whereas the drop's velocity and amplitude (maximum thickness) remain virtually unchanged. These conclusions have been confirmed by further studies, both numerical and analytical, for various models of CLs (Thiele *et al.* 2002; Schwartz, Roux & Cooper-White 2005; Koh *et al.* 2009; Savva & Kalliadasis 2013).

It should be noted, however, that 2D drops, just like many other two-dimensional liquid structures with CLs, are unstable with respect to transverse perturbations (e.g. Huppert 1982; Silvi & Dussan V. 1985; Jerrett & de Bruyn 1992; Bertozzi & Brenner 1997; Thiele & Knobloch 2003). As a result, 2D drops are never observed in nature.

Still, they have several important features in common with their 3D counterparts. In particular, sufficiently large 3D drops develop tails too, and an increase of the drop's mass beyond a certain threshold extends the tail but leaves the drop's amplitude and velocity unchanged (Podgorski, Flesselles & Limat 2001; Le Grand *et al.* 2005; Snoeijer *et al.* 2007). Thus, from a technical viewpoint, 2D drops could provide an excellent testing ground for mathematical methods to be later used for 3D drops.

In the present paper, we consider thin drops, both 2D and 3D, sliding down an inclined plate. The 2D case is examined under the sole assumption that the slip length l is much smaller than the drop's size. In the (more difficult) 3D case, we also assume that the Bond number is small and $\theta_r = \theta_a$.

The obtained expression for the drop's velocity is then tested against the experiments of Kim *et al.* (2002). It turns out that the theoretical and experimental results agree only for an unphysically small (subatomic) l. Given that our results are derived from the Navier-slip model, one has to conclude that it does not hold for glycerine, glycerine/water mixture and ethylene glycol used in the experiments of Kim *et al.* (2002). Recalling also that the experimental results of Podgorski *et al.* (2001), Winkels *et al.* (2011) and Puthenveettil *et al.* (2013) suggested a subatomic l for water and mercury, one might wonder whether the list of exceptions has become long enough to cast doubt on the actual rule.

At the same time, quite paradoxically, the theoretical dependence of the drop's velocity on the parameters other than l does agree with the experimental results, implying that the Navier-slip model can still be used for applications (albeit with an unphysically small l). This conclusion agrees with that of Limat (2014), who claimed that, even for water and mercury, the 'hydrodynamical model describes... logarithmic profiles, correlations between angles... reasonably well, but the price to be paid... seems to be the acceptance of an unphysical cutoff length scale'.

The results outlined above are presented as follows: in §2 we formulate the problem, in §§3 and 4 we examine 2D and 3D drops, and in §5 we compare our results with those of Kim *et al.* (2002).

2. Formulation of the problem

2.1. *The governing equations for 2D drops*

Consider a drop of liquid sliding down a plate inclined at an angle α. The liquid has density ρ, dynamic viscosity μ and surface tension σ, all of which are assumed to be constant in this investigation. We shall first formulate the governing equation for two spatial dimensions, so that the drop's thickness h_* depends on a single spatial coordinate x_* (with an axis directed down the plate – see figure 1).
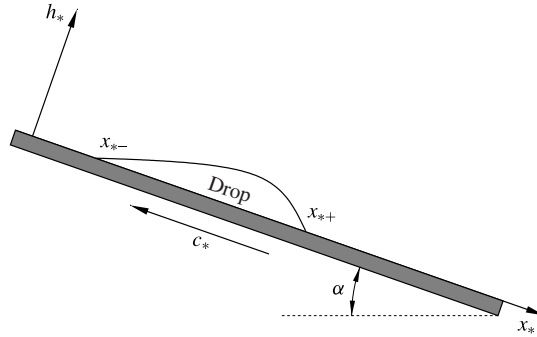
FIGURE 1. The setting (for the two-dimensional case): a drop sliding down an inclined plate.

This paper is concerned with drops steadily sliding with a constant velocity c_*, and it is convenient to assume that the plate is moving in the opposite direction with a matching velocity. In this case, the drop is stationary, and the coordinates $x_{*\pm}$ of its CLs are time-independent.

Let the drop's CLs be governed by the Navier-slip boundary condition. We shall also assume that the drop is thin and, thus, can be described by Hocking's (1981) lubrication equation. In application to a stationary drop on a moving plate, this equation reduces to

$$-c_* h_* + \left(\frac{h_*^3}{3} + l h_*^2 \right) \left(\frac{\sigma}{\mu} \frac{d^3 h_*}{dx_*^3} + \frac{\rho g \sin \alpha}{\mu} \right) = 0, \qquad (2.1)$$

where l is the slip length and g is the acceleration due to gravity.

We shall first assume that the advancing contact angle equals its receding counterpart, i.e. $\theta_a = \theta_r = \theta$, which corresponds to the following boundary conditions:

$$h_* \to 0, \quad \frac{dh_*}{dx_*} \to \mp \theta \quad \text{as} \ x_* \to x_{*\pm}. \qquad (2.2)$$

Having examined this particular case, we shall briefly discuss how the results obtained can be extended to Hocking's (1981) general model $\theta_r \neq \theta_a$ (see § 3.4).

Before non-dimensionalising the boundary-value problem (2.1) and (2.2), we note that it does not admit any solutions for the case of perfect wettability. Mathematically, this follows from the fact that, for $\theta = 0$, (2.1) does not have a real solution near the receding CL (see appendix A). Physically, the non-existence of a meaningful solution near $x = x_-$ reflects the fact that perfectly wetting liquids cannot recede, as they always leave behind a thin layer of liquid. Thus, the case $\theta = 0$ will not be examined in this work.

Now, we introduce the following non-dimensional variables:

$$x = \frac{x_*}{X}, \quad x_\pm = \frac{x_{*\pm}}{X}, \quad h = \frac{h_*}{H}, \quad c = \frac{c_*}{C}, \qquad (2.3a-d)$$

where

$$H = \left(\frac{\sigma \theta^3}{\rho g \sin \alpha} \right)^{1/2}, \quad X = \left(\frac{\sigma \theta}{\rho g \sin \alpha} \right)^{1/2}, \quad C = \frac{\sigma \theta^3}{\mu}. \qquad (2.4a-c)$$

These particular scales have been chosen to minimise the number of non-dimensional parameters left in the problem. It is also convenient to let

$$x_- = -XL, \quad x_+ = 0, \tag{2.5a,b}$$

where L is the drop's non-dimensional length.

By substituting (2.3)–(2.5) into (2.1) and (2.2) and omitting the asterisks, we obtain

$$\frac{\mathrm{d}^3 h}{\mathrm{d}x^3} = -1 + \frac{3c}{h(h+3\lambda)}, \tag{2.6}$$

$$h = 0, \quad \frac{\mathrm{d}h}{\mathrm{d}x} = 1 \quad \text{at } x = -L, \tag{2.7}$$

$$h = 0, \quad \frac{\mathrm{d}h}{\mathrm{d}x} = -1 \quad \text{at } x = 0, \tag{2.8}$$

where

$$\lambda = \frac{l}{H} \tag{2.9}$$

is the non-dimensional slip length. We observe that the *third*-order equation (2.6) is to be solved with *four* boundary conditions (2.7) and (2.8). As a result, for given λ and L, (2.6)–(2.8) determine both $h(x)$ and c (the latter is, essentially, the problem's eigenvalue).

Instead of the drop's length L, one can specify (as Hocking (1981) did) the drop's cross-sectional area

$$\int_{-L}^{0} h \, \mathrm{d}x = A, \tag{2.10}$$

and treat L as an unknown. Such an approach, however, implies mapping the *a priori* unknown domain $(-L, 0)$ into a domain with fixed boundaries. It has turned out that solving the problem for a given L and then calculating A is simpler.

2.2. *The governing equations for 3D drops*

In the 3D case, the non-dimensional governing equation can be written in the form

$$\nabla \left[-ch\boldsymbol{e}_x + \left(\frac{h^3}{3} + \lambda h^2 \right) (\boldsymbol{e}_x + \nabla \nabla^2 h) \right] = 0, \tag{2.11}$$

where $\boldsymbol{e}_x$ is the unit vector directed along the x axis (down the incline), and the y axis is implied to be horizontal and perpendicular to the x axis. Equation (2.11) can be rewritten in a more convenient form using an auxiliary function $\psi(x, y)$, such that

$$-ch + \frac{h^3}{3}\left(1 + \frac{\partial \nabla^2 h}{\partial x}\right) = -\frac{\partial \psi}{\partial y}, \quad \frac{h^3}{3}\frac{\partial \nabla^2 h}{\partial y} = \frac{\partial \psi}{\partial x}. \tag{2.12a,b}$$

These equations are to be solved with the following boundary conditions:

$$h = 0, \quad \psi = 0 \quad \text{at } \boldsymbol{r} = \boldsymbol{r}_c, \tag{2.13a,b}$$

$$\boldsymbol{n} \cdot \nabla h = 1 \quad \text{at } \boldsymbol{r} = \boldsymbol{r}_c, \tag{2.14}$$

where $\boldsymbol{r} = \boldsymbol{r}_c$ is a (parametric or other) representation of the CL and $\boldsymbol{n}$ is the inward unit normal to it. It should be noted that the boundary condition for ψ reflects the fact that the mass flux vanishes at the CL. The 3D equivalent of condition (2.10), in turn, is

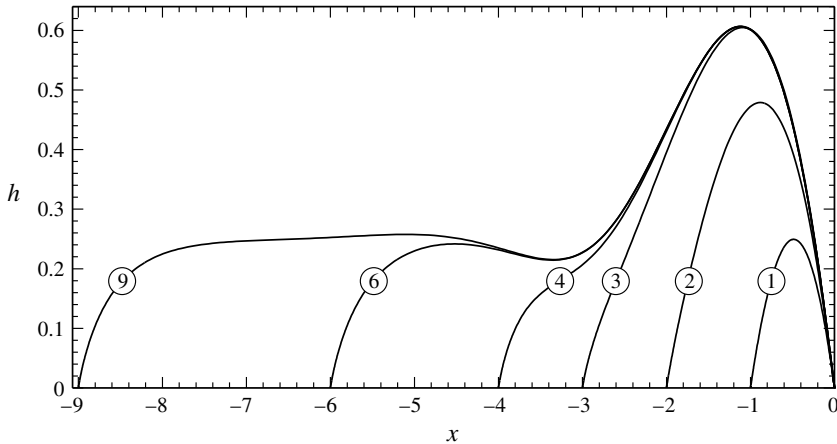$$\iint_B h \, \mathrm{d}x \, \mathrm{d}y = V, \tag{2.15}$$

FIGURE 2. Typical shapes of 2D drops (as computed using the boundary-value problem (2.6)–(2.8) with $\lambda = 0.001$). The curves are marked with the corresponding values of the drop length L.

where V is the drop's volume and B is the drop's base (i.e. the region bounded by the curve $\boldsymbol{r} = \boldsymbol{r}_c$).

2.3. *Classification of drops*

All results in this paper are based on the assumption that the non-dimensional slip length λ is small. Given this, three cases can be distinguished depending on the drop's non-dimensional horizontal size L (and, thus, the Bond number $Bo = L^2$):

  (i) small drops, $L \ll 1$;
 (ii) medium drops, $\lambda \ll L \sim 1$;
(iii) large drops, $L \gg 1$.

We observe that cases 1 and 2 overlap, with the non-overlapping part of the former, $L \lesssim \lambda$, being of little physical importance (the corresponding drops are too small). Thus, we shall only examine cases 2 and 3.

3. Two-dimensional drops

3.1. *The numerical results*

Before developing an asymptotic theory for the limit $\lambda \to 0$, it is helpful to compute some typical solutions of the boundary-value problem (2.6)–(2.8) and discuss their characteristic features.

The boundary-value problem (2.6)–(2.8) was solved numerically using the algorithm described in appendix B. A wide range of λ and L was explored.

Figure 2 shows examples of drops of increasing lengths. One can see that, by $L \approx 5$, the drop's front assumes a certain limiting shape which remains the same for all larger drops. One can also observe the 'tail' growing behind the frontal part (the same feature was observed by Hocking (1981), Savva & Kalliadasis (2013) and, in a slightly different formulation, by Thiele *et al.* (2002)).

It is instructive to plot the drop's global characteristics (such as the velocity, maximum thickness and cross-sectional area) as functions of the drop length – see figure 3.
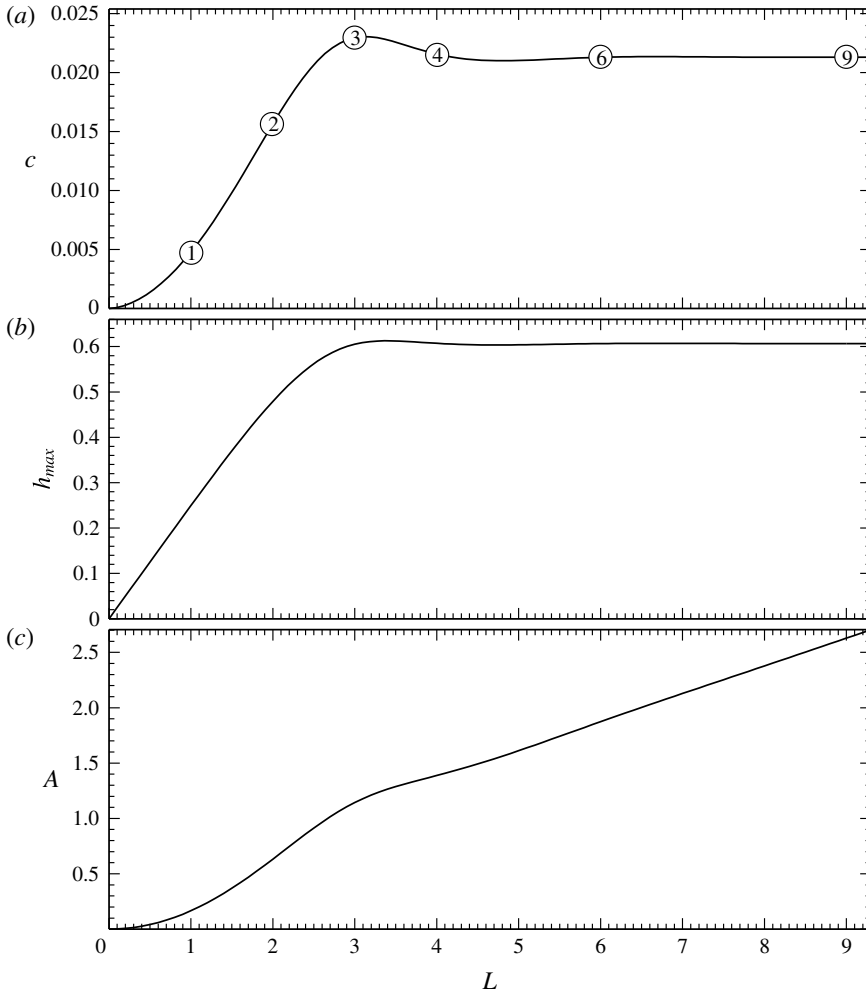
FIGURE 3. The dependence of a 2D drop's characteristics on its length L (as computed using the boundary-value problem (2.6)–(2.8) with $\lambda = 0.001$): (*a*) the velocity c, (*b*) the maximum thickness h_{max}, (*c*) the cross-sectional area A. The circled numbers in (*a*) indicate the corresponding values of L; the solutions with these values are shown in figure 2.

First, we observe that c is small, but not as small as λ (except for the smallest drops). In fact, a more precise estimate can be made,

$$c = O\left(\frac{1}{\ln \lambda}\right), \tag{3.1}$$

which will be confirmed by the asymptotic analysis below.

Second, for $L \gtrsim 5$, c and h_{max} are effectively constant. This suggests that the length of the tail does not affect the drop's global characteristics. One can also see that the tail is of virtually uniform thickness (later shown to approximately equal $\sqrt{3c}$), which agrees with the virtually linear dependence of A on L for $L \gtrsim 5$ (see figure 3*c*).

The observed features will be used as 'hints' when studying the solution's asymptotic structure. In particular, estimate (3.1) is the basis of all of our asymptotic results, both 2D and 3D.

3.2. *Medium drops*

The asymptotic structure of 2D medium drops involves an outer region and two boundary layers near the CLs.

The left boundary layer is described by the local variables

$$x_l = \frac{x+L}{\lambda}, \quad h_l = \frac{h}{\lambda}. \tag{3.2a,b}$$

In terms of (x_l, h_l), (2.6) and the left boundary condition (2.7) become

$$\frac{\mathrm{d}^3 h_l}{\mathrm{d}x_l^3} = \frac{3c}{h_l(h_l+3)} + O(\lambda^2), \tag{3.3}$$

$$h_l = 0, \quad \frac{\mathrm{d}h_l}{\mathrm{d}x_l} = 1 \quad \text{as } x_l \to 0. \tag{3.4}$$

We need two terms of the expansion of the solution in powers of c, for which (3.3) and (3.4) yield

$$h_l = x_l + a^{(1)}x^2 + c\left[\tfrac{1}{2}x_l^2 \ln x_l - \tfrac{1}{2}(x_l+3)^2 \ln(x_l+3) + \left(3\ln 3 + \tfrac{3}{2}\right)x_l + \tfrac{9}{2}\ln 3 + a^{(2)}x^2\right] + O(c^2). \tag{3.5}$$

It turns out that h_l does not match the outer solution unless $a^{(1)} = a^{(2)} = 0$; hence,

$$h_l = x_l + c\left[\tfrac{1}{2}x_l^2 \ln x_l - \tfrac{1}{2}(x_l+3)^2 \ln(x_l+3) + \left(3\ln 3 + \tfrac{3}{2}\right)x_l + \tfrac{9}{2}\ln 3\right] + O(c^2). \tag{3.6}$$

Next, the outer region is described by the unscaled variables. Accordingly, to match (3.6) to the outer solution, the former is to be expressed in terms of (x, h) and re-expanded in c,

$$h = (x+L) + 3c(x+L)[\ln \lambda - \ln(x+L) + \ln 3] + O(c^2). \tag{3.7}$$

Given estimate (3.1), one can see that the term $3c(x+L)\ln \lambda$ (originating from the first order of the inner solution) is now comparable to the term $(x+L)$ (originating from the zeroth order). It can be further shown that higher-order corrections to (3.6) include terms $O(c^n \ln^n x_l)$: if expressed through the outer variables, they contribute to the zeroth order of (3.7) and, thus, should all be taken into account when matching to the outer solution. This property of near-CL boundary layers was first observed by Hocking (1981), who also suggested a way of handling it (see also Voinov 1976; Lacey 1982; Sibley, Nold & Kalliadasis 2015).

First of all, we observe that, given estimate (3.1), the $O(\lambda^2)$ term in (3.3) is exponentially small and, thus, does not affect any order of our expansion (which is carried out in powers of c). Omitting this term, we introduce

$$\xi = c \ln x_l. \tag{3.8}$$

It is also convenient to replace h_l with

$$s = \frac{h_l}{x_l}. \tag{3.9}$$

In terms of (ξ, s), (3.3) becomes

$$-\frac{\mathrm{d}s}{\mathrm{d}\xi} + c^2 \frac{\mathrm{d}^3 s}{\mathrm{d}\xi^3} = \frac{3}{s(s + 3\mathrm{e}^{-\xi/c})}. \tag{3.10}$$

Keeping in mind that $\mathrm{e}^{-\xi/c}$ is exponentially small, one can readily verify that an asymptotic solution of (3.10) can be written in the form

$$s = (-9\xi + f_0 + cf_1)^{1/3} + O(c^2), \tag{3.11}$$

where f_0 and f_1 are constants of integration. Changing (ξ, s) back to (x_l, h_l), we obtain

$$h_l = x_l(-9c \ln x_l + f_0 + cf_1)^{1/3} + O(c^2). \tag{3.12}$$

Re-expanding (3.12) in c and matching the result to the large-x_l limit of (3.6), we obtain

$$f_0 = 1, \quad f_1 = 9 \ln 3. \tag{3.13a,b}$$

Finally, we use (3.2) to express solution (3.12)–(3.13) in terms of the unscaled variables, and then re-expand in c (with (3.1) kept in mind), which yields

$$h = (x + L) \left\{ \left(1 - 9c \ln \frac{1}{\lambda}\right)^{1/3} + \frac{3c[-\ln(x + L) + \ln 3]}{\left(1 - 9c \ln \frac{1}{\lambda}\right)^{2/3}} \right\} + O(c^2). \tag{3.14}$$

This asymptotics will play the role of a boundary condition for the outer solution, and a similar condition can be derived for the right boundary layer,

$$h = -x \left\{ \left(1 + 9c \ln \frac{1}{\lambda}\right)^{1/3} - \frac{3c[-\ln(-x) + \ln 3]}{\left(1 + 9c \ln \frac{1}{\lambda}\right)^{2/3}} \right\} + O(c^2). \tag{3.15}$$

To understand the physical meaning of the asymptotics (3.14) and (3.15), rewrite, say, the latter for $\mathrm{d}h/\mathrm{d}x$,

$$\frac{\mathrm{d}h}{\mathrm{d}x} = -\left(1 + 9c \ln \frac{1}{\lambda}\right)^{1/3} - \frac{3c[-\ln(-x) + \ln 3 + 1]}{\left(1 + 9c \ln \frac{1}{\lambda}\right)^{2/3}} + O(c^2). \tag{3.16}$$

This condition can be interpreted as a double-accuracy version of the Voinov–Hocking–Cox law (Voinov 1976; Hocking 1981; Hocking & Rivers 1982; Cox 1986) applied to the drop's front CL. The standard leading-order Hocking law corresponds to omitting the $O(c)$ term on the right-hand side of (3.16).

Before solving the outer problem, it is convenient to introduce

$$\varepsilon = \frac{1}{9 \ln \dfrac{1}{\lambda}}, \tag{3.17}$$

and rewrite (3.14) and (3.15) in the form

$$h \sim (x+L) \left\{ \left(1 - \frac{c}{\varepsilon}\right)^{1/3} + \frac{3c[-\ln(x+L) + \ln 3]}{\left(1 - \frac{c}{\varepsilon}\right)^{2/3}} \right\} + O(\varepsilon^2) \quad \text{as } x \to -L, \text{(3.18)}$$

$$h \sim -x \left\{ \left(1 + \frac{c}{\varepsilon}\right)^{1/3} - \frac{3c[-\ln(-x) + \ln 3]}{\left(1 + \frac{c}{\varepsilon}\right)^{2/3}} \right\} + O(\varepsilon^2) \quad \text{as } x \to 0. \quad \text{(3.19)}$$

We seek a solution of problem (2.6), (3.18) and (3.19) in the form

$$h = h^{(0)} + \varepsilon h^{(1)} + O(\varepsilon^2), \tag{3.20}$$

$$c = \varepsilon[c^{(0)} + \varepsilon c^{(1)} + O(\varepsilon^2)]. \tag{3.21}$$

In the zeroth order, we obtain

$$h^{(0)} = -\tfrac{1}{6}(x+M)(x+L)x, \tag{3.22}$$

where

$$M = \frac{6(1 + c^{(0)})^{1/3}}{L} \tag{3.23}$$

and the drop's leading-order velocity $c^{(0)}$ is related to its length L by

$$(1 + c^{(0)})^{1/3} - (1 - c^{(0)})^{1/3} = \tfrac{1}{6}L^2. \tag{3.24}$$

It turns out, however, that for $\lambda \geqslant 10^{-4}$, the leading-order results are not accurate enough, so we shall calculate $c^{(1)}$.

In the next-to-leading order, (2.6) and the asymptotic boundary conditions (3.18) and (3.19) yield

$$\frac{\mathrm{d}^3 h^{(1)}}{\mathrm{d}x^3} = \frac{3}{h^{(0)2}}, \tag{3.25}$$

$$h^{(1)} \sim (x+L)\frac{-c^{(1)} + 9c^{(0)}[-\ln(x+L) + \ln 3]}{3(1 - c^{(0)})^{2/3}} \quad \text{as } x \to -L, \tag{3.26}$$

$$h^{(1)} \sim -x\frac{c^{(1)} - 9c^{(0)}[-\ln(-x) + \ln 3]}{3(1 + c^{(0)})^{2/3}} \quad \text{as } x \to 0. \tag{3.27}$$

Upon substitution of expression (3.22) for $h^{(0)}$ into (3.25), it can be rewritten in terms of partial fractions,

$$\frac{\mathrm{d}^3 h^{(1)}}{\mathrm{d}x^3} = \frac{A_1}{x} + \frac{B_1}{x^2} + \frac{A_2}{x+L} + \frac{B_2}{(x+L)^2} + \frac{A_3}{x+M} + \frac{B_3}{(x+M)^2}, \tag{3.28}$$

where

$$A_1 = -\frac{216c^{(0)}(L+M)}{L^3 M^3}, \quad A_2 = \frac{216c^{(0)}(M - 2L)}{L^3(M-L)^3}, \quad A_3 = \frac{216c^{(0)}(2M - L)}{M^3(M-L)^3}, \quad \text{(3.29}a\text{–}c\text{)}$$

$$B_1 = \frac{108c^{(0)}}{L^2 M^2}, \quad B_2 = \frac{108c^{(0)}}{L^2(M-L)^2}, \quad B_3 = \frac{108c^{(0)}}{M^2(M-L)^2}. \quad \text{(3.30}a\text{–}c\text{)}$$
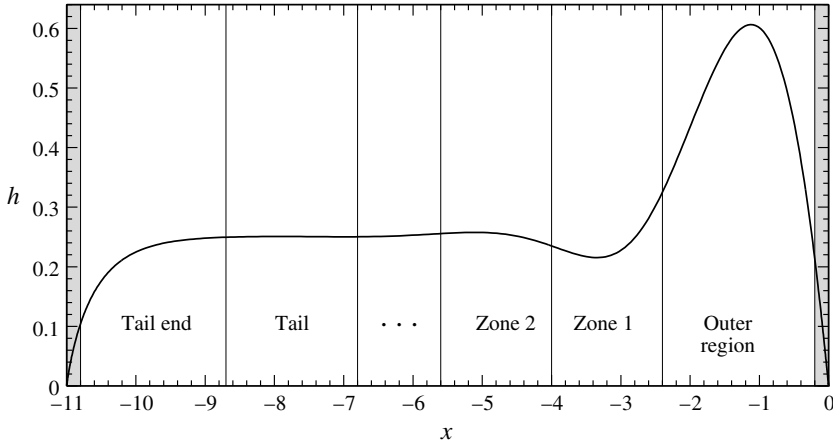
FIGURE 4. An illustration (for $\lambda = 0.001$, $L = 11$) of the asymptotic structure of the large-drop solution. Observe the small local maximum in Zone 2. The ellipsis '...' symbolises a (formally infinite) sequence of asymptotic zones representing alternating minima and maxima. The shaded regions are the left and right boundary layers.

By integrating (3.28) three times and matching the resulting solution to the asymptotics (3.26) and (3.27), we obtain, after some straightforward algebra,

$$\frac{c^{(1)}}{3}\left[\frac{1}{(1-c^{(0)})^{2/3}} + \frac{1}{(1+c^{(0)})^{2/3}}\right]$$
$$= 3(\ln 3 - 1)c^{(0)}\left[\frac{1}{(1-c^{(0)})^{2/3}} + \frac{1}{(1+c^{(0)})^{2/3}}\right] + 2(B_1 + B_2 + B_3) - (B_1 + B_2)\ln L$$
$$- \frac{A_3 M(M - L) - B_3(2M - L)}{L}\ln\left(1 - \frac{L}{M}\right) + \frac{(A_1 - A_2)L - A_3(2M - L)}{2}. \quad (3.31)$$

This equality relates the first-order velocity $c^{(1)}$ to the drop length L (we recall that M, $c^{(0)}$, $A_{1,2,3}$ and $B_{1,2,3}$ are related to L by (3.23)–(3.24) and (3.29)–(3.30)).

The physical meaning of the asymptotic results obtained for medium drops will be discussed in §3.4, after large drops have also been examined.

3.3. *Large drops*

The case of large drops is more complicated than its medium-drop counterpart, mostly due to the fact that it formally involves an infinite sequence of asymptotic zones. This feature was observed for the first time in a problem examined by Wilson & Jones (1983), and it has come up four times since then (Bowles 1995; Duchemin, Lister & Lange 2005; Benilov, Benilov & Kopteva 2008; Benilov *et al.* 2010). In all four cases, the infinite sequence of zones corresponds physically to a packet of short-scale ripples generated by gravity and surface tension. However, only one or two of the ripples (asymptotic zones) are typically visible in the exact solution, with the other zones being more of a mathematical abstraction. The present case is not an exception to this rule, as illustrated in figure 4.

Due to the similarity of (2.6) to the case examined by Benilov *et al.* (2008), we shall consider only the first two zones of the sequence: the outer region (describing
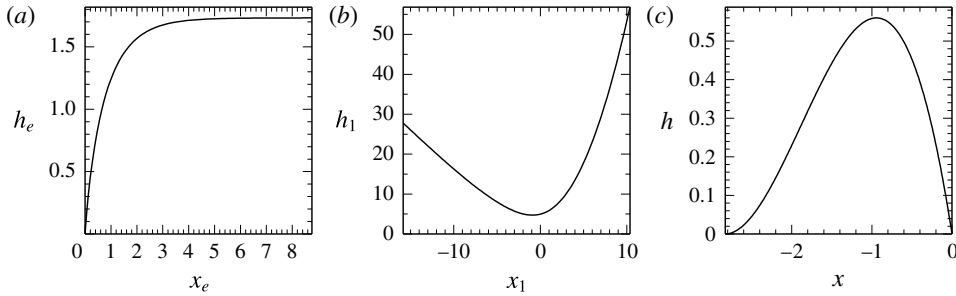
FIGURE 5. The solutions (for $\lambda = 0.001$) in the 'tail end' (*a*), in Zone 1 (*b*) and in the outer region (*c*).

the crest of a ripple) and Zone 1 (describing a trough). The rest of the sequence comprises alternating crests and troughs with decreasing amplitudes and widths, rapidly converging to a uniform 'tail' (see figure 4). These asymptotic zones will be examined in § 3.3.1, with the remaining two (the 'tail end' and the left boundary layer) examined in § 3.3.2.

3.3.1. *The drop's front*

It turns out that the velocity of a large drop is determined by the structure of the drop's rear. This makes the drop's front less important, so we shall calculate its shape with leading-order accuracy only.

The outer region is described by the 'natural' (non-scaled) variables (x, h). Given that we still expect c to be small, the original (2.6) in this case reduces, to leading order, to

$$\frac{\mathrm{d}^3 h}{\mathrm{d}x^3} = -1. \tag{3.32}$$

As in the case of a medium drop, the outer region can be matched to the right boundary layer only if we require

$$h = 0 \quad \text{at } x = 0. \tag{3.33}$$

The left boundary condition, however, cannot be enforced for the outer region (since $L \gg 1$, the left boundary is too far away). It turns out that the outer solution can be matched to the neighbouring zone to its left only if $h(x)$ approaches the x-axis at a zero angle, which corresponds to the following solution of (3.32) and (3.33):

$$h = -\tfrac{1}{6}(x + W)^2 x, \tag{3.34}$$

where W is the width of the drop's 'main body', and it also determines the amplitude of the drop,

$$h_{max} = \tfrac{2}{81} W^3. \tag{3.35}$$

Solution (3.34) is illustrated in figure 5(*c*).

The right boundary layer should be handled in the same way as it was in the medium-drop case, which yields, at leading order,

$$\frac{1}{6} W^2 = \left(1 + 9c \ln \frac{1}{\lambda} \right)^{1/3}. \tag{3.36}$$

Given relationship (3.35) between h_{max} and W, this equality relates the (large) drop's amplitude to its velocity.

Zone 1 is described by the local variables (x_1, h_1), such that

$$x = -W + c^{1/3}x_1, \quad h = c^{2/3}h_1, \tag{3.37a,b}$$

for which (2.6), to leading order, becomes

$$\frac{\mathrm{d}^3 h_1}{\mathrm{d}x_1^3} = \frac{3}{h_1^2}. \tag{3.38}$$

Taking the limit $x \to -W$ of the outer solution (3.34), one can deduce that (3.34) matches $h_1(x_1)$ only if

$$h_1 \sim \tfrac{1}{6}Wx_1^2 \quad \text{as } x_1 \to \infty. \tag{3.39}$$

Next, it can be verified that $h_1(x_1)$ matches the solution in Zone 2 only if it has the following asymptotic behaviour:

$$h_1 \sim -x_1(9\ln x_1)^{1/3} \quad \text{as } x_1 \to -\infty. \tag{3.40}$$

The solution of the eigenvalue problem (3.38)–(3.40) was computed numerically (see figure 5*b*). As mentioned before, it describes a dip in the drop's surface, and is flanked by two peaks: the outer region on the right and a much smaller peak on the left (in figure 4, the latter is labelled 'Zone 2').

Finally, the 'tail' is described by the following solution of (2.6):

$$h = (3c)^{1/2} + O(\lambda). \tag{3.41}$$

3.3.2. *The drop's rear*

The 'tail end' (see figure 4) is described by the local variables (x_e, h_e),

$$x = -L + c^{1/6}x_e, \quad h = c^{1/2}h_e. \tag{3.42a,b}$$

By rewriting (2.6) in terms of (x_e, h_e) and keeping the leading order only, we obtain

$$\frac{\mathrm{d}^3 h_e}{\mathrm{d}x_e^3} = -1 + \frac{3}{h_e^2}. \tag{3.43}$$

To match $h_e(x_e)$ to the tail solution (3.41), we require

$$h_e \to 3^{1/2} \quad \text{as } x_e \to \infty. \tag{3.44}$$

It turns out that $h_e(x_e)$ matches the left boundary layer (to be examined below) only if

$$h_e \to 0 \quad \text{as } x_e \to 0. \tag{3.45}$$

The solution of problem (3.43)–(3.45) was computed numerically (see §C.2), and it is shown in figure 5(*a*).

It should be noted also that, as demonstrated in §C.1, h_e has the following asymptotics:

$$h_e = -x_e \left\{ (9\ln x_e)^{1/3} + \frac{b}{(9\ln x_e)^{2/3}} + O\left[\frac{\ln(-\ln x_e)}{\ln^{5/3}x_e}\right] \right\} \quad \text{as } x_e \to 0. \tag{3.46}$$

Within the framework of this asymptotics, the constant b remains arbitrary, as it is determined by the global solution of problem (3.43)–(3.45). The method for computing b is described in §C.3 and it yields

$$b \approx -0.613. \tag{3.47}$$

The left boundary layer for large drops is exactly the same as its medium-drop counterpart, i.e. is represented by expression (3.6). To match it to the asymptotics (3.46) of the tail end, we use (3.42) and (3.2) to deduce

$$x_e = \frac{\lambda x_l}{c^{1/6}}, \qquad h_e = \frac{\lambda h_l}{c^{1/2}}. \tag{3.48a,b}$$

Expressing then (3.46) in terms of (x_l, h_l) and taking advantage of estimate (3.1), we obtain

$$h_l \sim -x_l (9c \ln \lambda)^{1/3} \left(1 - \frac{\ln c}{18 \ln \lambda} + \frac{\ln x_l}{3 \ln \lambda} + \frac{b}{9 \ln \lambda} + O\left[\frac{\ln(-\ln \lambda)}{\ln^2 \lambda} \right] \right). \tag{3.49}$$

We also expand the dependence of c on λ,

$$c = \frac{c_1}{\ln \dfrac{1}{\lambda}} + \frac{c_2 \ln(-\ln \lambda) + c_3}{\ln^2 \dfrac{1}{\lambda}} + O\left[\frac{\ln^2(-\ln \lambda)}{\ln^3 \dfrac{1}{\lambda}} \right], \tag{3.50}$$

where c_1, c_2 and c_3 are order-one coefficients. On substituting (3.50) into (3.49) and (3.6), and matching these, we obtain

$$c_1 = \tfrac{1}{9}, \quad c_2 = -\tfrac{1}{54}, \quad c_3 = \tfrac{1}{27}(b + 4 \ln 3). \tag{3.51a-c}$$

Thus, expression (3.50) becomes

$$c = \frac{1}{9 \ln \dfrac{1}{\lambda}} + \frac{\ln(-\ln \lambda)}{54 \ln^2 \dfrac{1}{\lambda}} + \frac{b + 4 \ln 3}{27 \ln^2 \dfrac{1}{\lambda}} + O\left[\frac{\ln^2(-\ln \lambda)}{\ln^3 \lambda} \right], \tag{3.52}$$

where it should be recalled that b is given by (3.47).

3.4. *Discussion*

(i) The velocity of medium drops (determined by (3.21), (3.17), (3.24), (3.31)) and that of large drops (given by (3.52)) are compared with the numerical solution of the exact boundary-value problem (2.6)–(2.8) in figure 6. One can see that the numerical and asymptotic results agree reasonably well, especially since the latter are based on expansions in *logarithmically* small parameters.

The high accuracy of the results obtained should be attributed to the fact that c has been calculated to the first order. The leading-order results, in turn, are not sufficiently accurate for $\lambda \geqslant 10^{-4}$ (see figure 6).

(ii) It is instructive to adapt the medium-drop results to the limit of small Bond number. By assuming $L^2 \ll 1$ in (3.21) and expression (3.24), substituting the resulting $c^{(0)}$ and $c^{(1)}$ into (3.31), and recalling definition (3.17) of ε, we obtain

$$c = \frac{1}{9 \ln \dfrac{1}{\lambda}} \left[\frac{L^2}{4} + O(L^6) \right] + \frac{1}{81 \ln^2 \dfrac{1}{\lambda}} \left[\frac{9}{4} L^2 \ln \frac{3}{L} + O(L^4 \ln L) \right] + O\left(\frac{1}{243 \ln^3 \dfrac{1}{\lambda}} \right). \tag{3.53}$$
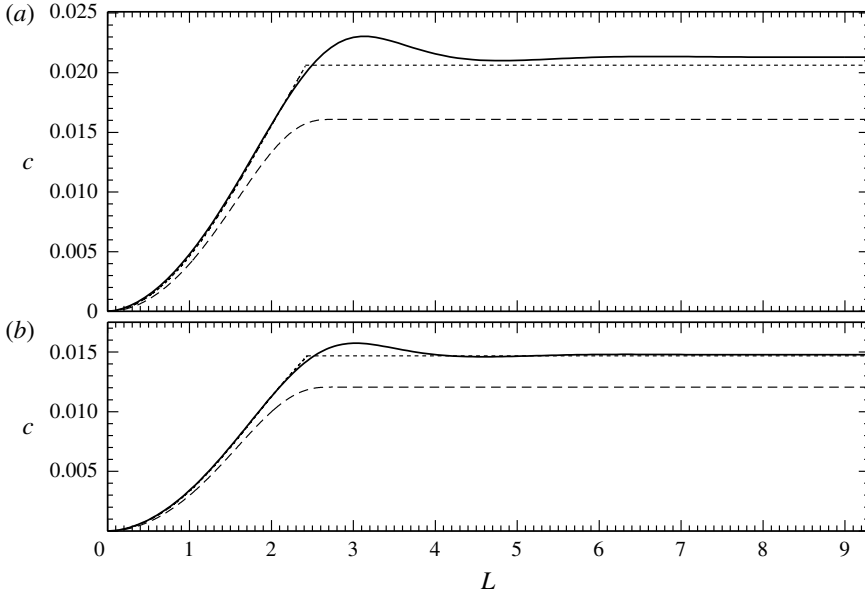
FIGURE 6. The numerical (solid line), zeroth-order asymptotic (dashed line) and first-order asymptotic (dotted line) dependences of the velocity c of a 2D drop on its length L, for $\lambda = 0.001$, 0.0001. The sloping and horizontal dashed/dotted lines represent the asymptotic results for medium and large drops respectively.
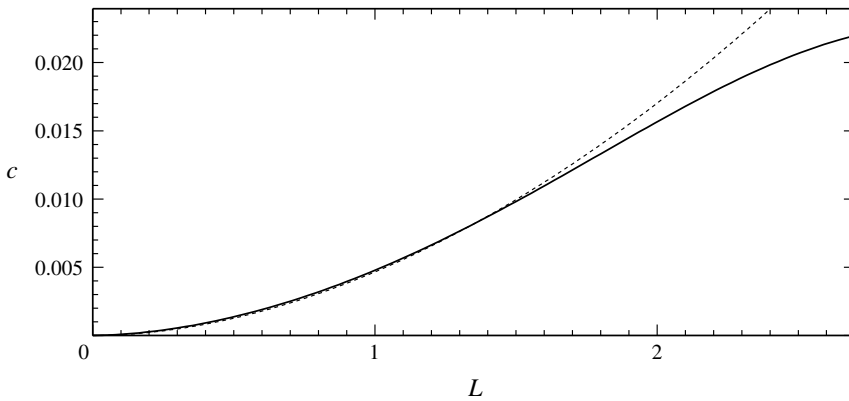

FIGURE 7. The numerical (solid line) and first-order small-Bond-number asymptotic (dotted line) dependences of the velocity c of a 2D drop on its length L, for $\lambda = 0.001$ and medium drops.

Figure 7 shows that, even though this expression has been formally obtained for small L, it is reasonably accurate for $L \lesssim 2$.

(iii) Medium 2D drops have been examined previously by Savva & Kalliadasis (2013) using a model similar to our (2.1), but with an extra term describing the hydrostatic pressure gradient (which becomes important in the limit $\alpha \ll 1$, i.e. if the plate's slope is small). It can be readily shown that, if $\alpha \sim 1$, our leading-order medium-drop results agree with those of Savva & Kalliadasis (2013).

(iv) We observe that the asymptotic results for medium/large drops (shown by the sloping/horizontal dotted lines in figure 6) do not form a smooth junction. This indicates that there exists an intermediate region where neither approximation works.

This 'gap' is a result of the requirement that the parameter M in expression (3.22) must exceed the drop length L, otherwise the drop thickness becomes negative for some x, as does the apparent contact angle at the rear CL. As follows from (3.22) and (3.23), the marginal case $M = L$ corresponds to

$$L = 3^{1/2}2^{2/3} \approx 2.75. \tag{3.54}$$

Thus, the medium-drop asymptotic results are valid only for $L \lesssim 3^{1/2}2^{2/3}$. The large-drop results, in turn, are valid for $L \gg 1$, which clearly leaves a gap where neither approximation is applicable.

In principle, the gap can be bridged by considering several intermediate limits (starting from $L \approx 3^{1/2}2^{2/3}$). These limits, however, involve a large amount of tedious algebra. Thus, since the results obtained capture the problem's most important qualitative features (the quadratic nature of $c(L)$ for $L \ll 1$ and the existence of the limiting velocity for $L \gg 1$), there seems to be little urgency in exploring the intermediate limits.

(v) We recall that the expression for the velocity of large drops is fully determined by matching of the tail end and left boundary layer, i.e. it is not affected by other asymptotic zones. This comes as a surprise, as one would intuitively assume a drop's velocity to depend on the parameters of the advancing CL or both CLs. This feature indicates the importance of the tail for the dynamics of large drops.

In fact, if one is concerned with the velocity of a large drop and not its shape, one could use (2.6) with the boundary condition describing the left boundary layer,

$$h \to 0, \quad \frac{\mathrm{d}h}{\mathrm{d}x} \to 1 \quad \text{as } x \to -L, \tag{3.55}$$

and the tail end,

$$h \to \text{const.} \quad \text{as } x \to \infty. \tag{3.56}$$

For $L \gg 1$, the boundary-value problem (2.6), (3.55) and (3.56) yields c which is very close to that of the original problem (2.6)–(2.8). For $L \geqslant 6$ (and $\lambda = 10^{-3}$), for example, the two values of c differ by less than 10^{-5}.

(vi) As mentioned before, Hocking (1981) examined a more general problem, with the boundary conditions (2.2) replaced by

$$h \to 0, \quad \frac{\mathrm{d}h}{\mathrm{d}x} \to \theta_r \quad \text{as } x \to x_-, \tag{3.57}$$

$$h \to 0, \quad \frac{\mathrm{d}h}{\mathrm{d}x} \to -\theta_a \quad \text{as } x \to x_+. \tag{3.58}$$

Letting the parameter θ used in the non-dimensionalisation (2.3) and (2.4) be $\theta = (\theta_r + \theta_a)/2$, we can write the modified version of the non-dimensional boundary conditions in the form

$$h \to 0 = \begin{cases} \dfrac{\mathrm{d}h}{\mathrm{d}x} \to \theta_- & \text{as } x \to -L, \\ \dfrac{\mathrm{d}h}{\mathrm{d}x} \to -\theta_+ & \text{as } x \to 0, \end{cases} \tag{3.59}$$

where

$$\theta_- = \frac{2\theta_r}{\theta_r + \theta_a}, \quad \theta_+ = \frac{2\theta_a}{\theta_r + \theta_a}. \tag{3.60a,b}$$

The analysis of the boundary-value problem (2.6), (3.59) is very similar to that in the case $\theta_r = \theta_a$, and it will not be presented in detail. We shall only summarise the leading-order results for the drop's velocity (the next-to-leading-order ones can be obtained in a similar fashion). For a medium drop, $c^{(0)}$ satisfies

$$(\theta_-^3 + c^{(0)})^{1/3} - (\theta_+^3 - c^{(0)})^{1/3} = \tfrac{1}{6}L^2 \tag{3.61}$$

(compare this equation with (3.24), which implies $\theta_+ = \theta_- = 1$). For large drops, in turn, we have

$$c^{(0)} = \frac{\theta_-}{9 \ln \dfrac{1}{\lambda}}. \tag{3.62}$$

This expression is a generalisation of the first term in expansion (3.52).

4. Three-dimensional drops

The structure of the solution in this case is similar to that of 2D drops: it involves the central (outer) region and a narrow boundary layer near the CL. Since the width of the boundary layer is much smaller than the drop's size, the boundary layer is essentially two-dimensional. As before, we shall first neglect the hysteresis interval (i.e. assume $\theta_r = \theta_a$), with the general case discussed briefly in § 5.2.

Thus, the exact boundary condition (2.14) can be replaced with a 3D equivalent of the asymptotics (3.16) – such that dh/dx is replaced with $-\boldsymbol{n} \cdot \boldsymbol{\nabla} h$ and c is replaced with the projection of the drop's velocity onto the normal vector, i.e. $c\boldsymbol{n} \cdot \boldsymbol{e}_x$,

$$
\boldsymbol{n} \cdot \boldsymbol{\nabla} h = \left(1 + 9c\boldsymbol{n} \cdot \boldsymbol{e}_x \ln \frac{1}{\lambda}\right)^{1/3}
$$
$$
+ \frac{3c\boldsymbol{n} \cdot \boldsymbol{e}_x[-\ln(-x) + \ln 3 + 1]}{\left(1 + 9c\boldsymbol{n} \cdot \boldsymbol{e}_x \ln \dfrac{1}{\lambda}\right)^{2/3}} + O(c^2) \quad \text{at } r = r_c. \tag{4.1}
$$

In what follows, we carry out all calculations to the leading order only, which implies that the terms $O(c)$ in (4.1) and the governing equations (2.12) should be omitted. Rewriting the truncated versions of (2.12), (4.1), the boundary conditions (2.13) and the volume condition (2.15) in terms of the polar coordinates (r, ϕ), we obtain

$$\frac{h^3}{3}\left(\cos \phi + \frac{\partial \nabla^2 h}{\partial r}\right) = -\frac{1}{r}\frac{\partial \psi}{\partial \phi}, \quad \frac{h^3}{3}\left(-\sin \phi + \frac{1}{r}\frac{\partial \nabla^2 h}{\partial \phi}\right) = \frac{\partial \psi}{\partial r}, \tag{4.2a,b}$$

$$\frac{\dfrac{1}{r}\dfrac{dR}{d\phi}\dfrac{\partial h}{\partial \phi} - R\dfrac{\partial h}{\partial r}}{\sqrt{\left(\dfrac{dR}{d\phi}\right)^2 + R^2}} = \left[1 + 3\hat{c}\frac{\dfrac{dR}{d\phi}\sin \phi + R \cos \phi}{\sqrt{\left(\dfrac{dR}{d\phi}\right)^2 + R^2}}\right]^{1/3} \quad \text{at } r = R(\phi), \tag{4.3}$$

$$h = 0, \quad \psi = 0 \quad \text{at } r = R(\phi), \tag{4.4a,b}$$

$$\int_0^\infty \int_0^{2\pi} h\, r\, dr\, d\phi = V, \tag{4.5}$$

where

$$\hat{c} = 3c \ln \frac{1}{\lambda} \tag{4.6}$$

and $r = R(\phi)$ is the polar representation of the CL. The boundary-value problem (4.2)–(4.6) is still not simple enough to be solved analytically. We shall solve (4.2)–(4.6) asymptotically, in the limit of small R (or, equivalently, small Bond number).

Since small R implies that the drop's volume V is also small, it is convenient to introduce

$$\delta = \left(\frac{4V}{\pi} \right)^{1/3} \tag{4.7}$$

and rescale the variables as follows:

$$r_{new} = \frac{r}{\delta}, \quad \phi_{new} = \phi, \tag{4.8a,b}$$

$$h_{new} = \frac{h}{\delta}, \quad \psi_{new} = \frac{\psi}{\delta^2}, \quad R_{new} = \frac{R}{\delta}, \quad \hat{c}_{new} = \frac{\hat{c}}{\delta^2} \tag{4.9a-d}$$

(observe that the scaling of $\hat{c}$ implies that small drops slide slowly). Substituting (4.8) and (4.9) into (4.2)–(4.5) and omitting the subscript $_{new}$, we obtain

$$\frac{h^3}{3} \left(\delta^2 \cos\phi + \frac{\partial \nabla^2 h}{\partial r} \right) = -\frac{1}{r} \frac{\partial \psi}{\partial \phi}, \quad \frac{h^3}{3} \left(-\delta^2 \sin\phi + \frac{1}{r} \frac{\partial \nabla^2 h}{\partial \phi} \right) = \frac{\partial \psi}{\partial r}, \tag{4.10a,b}$$

$$\frac{1}{R^2} \frac{\mathrm{d}R}{\mathrm{d}\phi} \frac{\partial h}{\partial \phi} - \frac{\partial h}{\partial r} = \sqrt{1 + \left(\frac{1}{R} \frac{\mathrm{d}R}{\mathrm{d}\phi} \right)^2}$$
$$+ \delta^2 \hat{c} \left(\frac{1}{R} \frac{\mathrm{d}R}{\mathrm{d}\phi} \sin\phi + \cos\phi \right) + O(\delta^4) \quad \text{at } r = R(\phi), \tag{4.11}$$

$$h = 0, \quad \psi = 0 \quad \text{at } r = R(\phi), \tag{4.12a,b}$$

$$\int_0^{2\pi} \int_0^R h r \, \mathrm{d}r \, \mathrm{d}\phi = \frac{\pi}{4}. \tag{4.13}$$

We seek a solution in the form

$$h = h^{(0)} + \delta^2 h^{(1)} + \cdots, \quad \psi = \psi^{(0)} + \delta^2 \psi^{(1)} + \cdots, \tag{4.14a,b}$$

$$R = R^{(0)} + \delta^2 R^{(1)} + \cdots, \quad \hat{c} = \hat{c}^{(0)} + \cdots. \tag{4.15a,b}$$

Expanding (4.10)–(4.13) to leading order, one can deduce that

$$R^{(0)} = 1, \quad h^{(0)} = \tfrac{1}{2}(1 - r^2), \quad \psi^{(0)} = 0. \tag{4.16a-c}$$

In the next order, (4.10)–(4.13) yield

$$h^{(0)2} h^{(1)} \frac{\partial \nabla^2 h^{(0)}}{\partial r} + \frac{h^{(0)3}}{3} \left(\cos\phi + \frac{\partial \nabla^2 h^{(1)}}{\partial r} \right) = -\frac{1}{r} \frac{\partial \psi^{(1)}}{\partial \phi}, \tag{4.17}$$

$$\frac{h^{(0)3}}{3} \left(-\sin\phi + \frac{1}{r} \frac{\partial \nabla^2 h^{(1)}}{\partial \phi} \right) = \frac{\partial \psi^{(1)}}{\partial r}, \tag{4.18}$$

$$-\frac{\partial h^{(1)}}{\partial r} - \frac{\partial^2 h^{(0)}}{\partial r^2} R^{(1)} = \hat{c}^{(0)} \cos\phi \quad \text{at } r = 1, \tag{4.19}$$

$$h^{(1)} + \frac{\partial h^{(0)}}{\partial r} R^{(1)} = 0, \quad \psi^{(1)} + \frac{\partial \psi^{(0)}}{\partial r} R^{(1)} = 0 \quad \text{at } r = 1, \tag{4.20a,b}$$

$$\int_0^{2\pi} \int_0^1 h^{(1)} r \, \mathrm{d}r \, \mathrm{d}\phi = 0. \tag{4.21}$$

Seeking the solution of these equations in the form

$$h^{(1)}(r,\phi) = \hat{h}^{(1)}(r) \cos\phi, \quad \psi^{(1)}(r,\phi) = \hat{\psi}^{(1)}(r) \sin\phi, \quad R^{(1)}(\phi) = \hat{R}^{(1)} \cos\phi, \tag{4.22a-c}$$

then taking into account expressions (4.24), and eventually eliminating $R^{(1)}$, we obtain

$$\frac{\mathrm{d}}{\mathrm{d}r} \left[\frac{1}{r} \frac{\mathrm{d}}{\mathrm{d}r} \left(r \frac{\mathrm{d}\hat{h}^{(1)}}{\mathrm{d}r} \right) - \frac{1}{r^2} \hat{h}^{(1)} \right] + \frac{24}{r(1-r^2)^3} \hat{\psi}^{(1)} = -1, \tag{4.23}$$

$$\frac{1}{r} \left[\frac{1}{r} \frac{\mathrm{d}}{\mathrm{d}r} \left(r \frac{\mathrm{d}\hat{h}^{(1)}}{\mathrm{d}r} \right) - \frac{1}{r^2} \hat{h}^{(1)} \right] + \frac{24}{(1-r^2)^3} \frac{\mathrm{d}\hat{\psi}^{(1)}}{\mathrm{d}r} = -1, \tag{4.24}$$

$$-\frac{\mathrm{d}\hat{h}^{(1)}}{\mathrm{d}r} + \hat{h}^{(1)} = \hat{c}^{(0)}, \quad \hat{\psi}^{(1)} = 0 \quad \text{at } r = 1. \tag{4.25a,b}$$

It is convenient to introduce

$$F = \frac{\mathrm{d}^2 \hat{h}^{(1)}}{\mathrm{d}r^2} + \frac{1}{r} \frac{\mathrm{d}\hat{h}^{(1)}}{\mathrm{d}r} - \frac{1}{r^2} \hat{h}^{(1)}, \tag{4.26}$$

which allows one to eliminate $\psi^{(1)}$ from (4.23)–(4.25) and decouple F from $\hat{c}^{(0)}$,

$$r^2(1-r^2) \frac{\mathrm{d}^2 F}{\mathrm{d}r^2} + r(1-7r^2) \frac{\mathrm{d}F}{\mathrm{d}r} - (1-r^2)F = 7r^3 - r^2 - r + 1, \tag{4.27}$$

$$F \sim \text{const.} \quad \text{as } r \to 1, \tag{4.28}$$

$$F \sim -1 - \tfrac{1}{2} r \ln r \quad \text{as } r \to 0 \tag{4.29}$$

and

$$\hat{c}^{(0)} = - \int_0^1 r^2 F \, \mathrm{d}r. \tag{4.30}$$

The boundary-value problem (4.27)–(4.29) has been solved numerically (by shooting) and the integral in (4.30) was evaluated to yield

$$\hat{c}^{(0)} \approx 0.48501. \tag{4.31}$$

Recalling scaling (4.9) of $\hat{c}$, relationship (4.6) of $\hat{c}$ to the non-dimensional velocity c, definition (4.7) of δ, and non-dimensionalisation (2.3) and (2.4), we obtain for the drop's dimensional velocity

$$c_* \approx 0.18992 \frac{V_*^{2/3} \theta^{4/3} \rho g \sin\alpha}{\mu \ln \dfrac{X}{l}}, \tag{4.32}$$

where V_* is the dimensional volume and X is defined by (2.4).

Expression (4.32) is the main result of the present paper.

5. Discussion

5.1. *Comparison with the results of Kim et al. (2002)*

Kim *et al.* (2002), hereafter referred to as KLK02, examined the energy balance of drops sliding down an inclined plate and obtained a qualitative estimate for their velocity. As many qualitative estimates do, this one involves an undetermined non-dimensional constant.

In what follows, this constant will be fixed by adapting the estimate of KLK02 to the thin-drop limit and matching the result to our expression (4.32). Once the constant is determined, it can be used in the original estimate for arbitrary drops, turning it into a quantitative formula. This plan is best understood through an analogy with an outer asymptotic solution involving undetermined parameters which can be fixed through matching with the inner solution.

KLK02 obtained the following expression for the dimensional velocity:

$$c_* \approx \gamma \frac{\rho g}{\mu c(\theta) s(\theta)} \frac{V_*^{2/3}(\sin\alpha - \sin\alpha_c)}{\ln \dfrac{R_b}{l}}, \qquad (5.1)$$

where γ is an undetermined constant, V_* is the drop's dimensional volume, α_c is the critical value of the inclination angle α (such that, for $\alpha < \alpha_c$, the drop remains static), R_b is the radius of the drop's base and

$$c(\theta) = \frac{2\theta \sin^2\theta - \frac{1}{2}\sin 2\theta + \frac{1}{4}\sin 4\theta}{(\sin 2\theta - 2\theta)^2}, \quad s(\theta) = \frac{2^{4/3}\sin\theta}{3^{1/3}(1 - \cos\theta - \frac{1}{2}\cos\theta\,\sin^2\theta)^{1/3}}. \tag{5.2a,b}$$

In order to adapt expression (5.1) to the case of thin drops, we observe that

$$c(\theta) \sim \tfrac{3}{4}\theta^{-1}, \quad s(\theta) \sim 2^{4/3}3^{-1/3}\theta^{-1/3} \quad \text{as } \theta \to 0. \tag{5.3a,b}$$

It should be noted also that, unlike us, KLK02 assumed different values for the advancing and receding contact angles (which is why they have $\alpha_c \neq 0$). The advantages/shortcomings of the two models will be discussed later, whereas here we simply adapt the results of KLK02 to our assumptions, i.e. set

$$\alpha_c = 0. \tag{5.4}$$

We also assume that the ratio of R_b to our spatial scale X (defined by (2.4)) is much smaller than the ratio of either of them to the slip length l, which implies that

$$\ln \frac{R_b}{l} \approx \ln \frac{X}{l}. \tag{5.5}$$

Substitution of (5.3)–(5.5) into (5.1) yields

$$c_* \approx \frac{\gamma}{2^{-2/3}3^{2/3}} \frac{\rho g \sin\alpha}{\mu \ln \dfrac{X}{l}} V_*^{2/3}\theta^{4/3}. \tag{5.6}$$

This expression has exactly the same dependence on the physical parameters as that of our expression (4.32), which should be viewed as an extra validation for both results.

Source	Liquid	γ
KLK02	Glycerine	1.1×10^{-2}
KLK02	Ethylene glycol	1.3×10^{-2}
KLK02	Water/glycerine mixture	1.8×10^{-2}
PSH13	Water	4×10^{-2}
PSH13	Mercury	4×10^{-2}

TABLE 1. The experimental values of the coefficient γ from expression (5.1) extracted from the results of KLK02 (Kim *et al.* 2002) and PSH13 (Puthenveettil *et al.* 2013), for various liquids.

Furthermore, comparing (5.6) with (4.32), one can deduce that

$$\gamma \approx 0.24887. \tag{5.7}$$

With γ given by (5.7), formula (5.1) becomes a quantitative result (and it is still valid for thick drops, of course).

It is interesting to compare the theoretical value (5.7) with the experimental ones obtained by KLK02 and Puthenveettil *et al.* (2013) (the latter work will be referred to as PSH13). It should be noted that both papers assume

$$l \sim 10^{-8} \text{ m}. \tag{5.8}$$

The values of γ extracted from the results of KLK02 and PSH13 are presented in table 1. We observe that the values obtained for different liquids differ from each other by a factor of up to 3.6, and even the largest one is smaller than the theoretical value (5.7) by a factor of more than 7. In principle, an agreement between the experimental and theoretical results can be achieved by assuming a value of l different from (5.8), but, practically, this does not work because l becomes unphysically small (subatomic).

We conclude that the Navier-slip model of CLs (from which our results have been derived) does not hold for glycerine, glycerine/water mixture or ethylene glycol (used in the experiments of Kim *et al.* 2002). Recalling also that Podgorski *et al.* (2001), Winkels *et al.* (2011) and Puthenveettil *et al.* (2013) observed unphysically small l for water and mercury, one cannot help wondering whether the Navier-slip model has sound physical foundations.

At the same time, quite paradoxically, the dependence of our results on the parameters other than l does agree with the results of Kim *et al.* (2002). This conclusion agrees with that of Limat (2014), who claimed that the 'hydrodynamical model describes... logarithmic profiles, correlations between angles... reasonably well, but the price to be paid... seems to be the acceptance of an unphysical cutoff length scale'.

This suggests that, until a physically consistent model of CLs is developed, the Navier-slip model (with an unphysically small l) can still be used in, say, industrial applications.

5.2. *The effect of the hysteresis interval*

It should be noted that our approach (as well as that of all researchers assuming $\theta_a = \theta_r$) implies that drops slide for all values of the inclination angle α. Experiments,
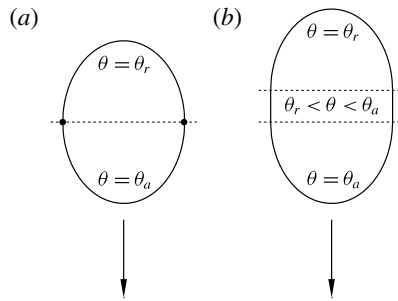
FIGURE 8. A 3D drop viewed from above (a schematic). The arrow shows the direction of motion. (*a*) If all of the CL is curved, two points exist (shown by black dots) where the contact angle changes abruptly from its receding value θ_r to its advancing value θ_a. (*b*) To resolve the singularity, two straight segments should be introduced to the CL, along which θ changes continuously from θ_r to θ_a.

on the other hand, show that, for most liquid/substrate combinations, there exists a critical value α_c such that, if $\alpha < \alpha_c$, the drop remains static. This is usually attributed to the existence of a hysteresis interval, i.e. a range of contact angles for which the CL remains static.

This seems to imply that our results are valid only if the hysteresis interval is narrow, and, even though such materials do exist (e.g. Glassmaker *et al.* 2007; Smith *et al.* 2013), it is still a restriction.

Models involving hysteresis, however, are associated with a certain difficulty.

Indeed, even though they work well in two dimensions, for 3D drops they appear to give rise to singularities at the points where the tangent to the CL is parallel to the drop's velocity (see figure 8*a*). At such points, a model with $\theta_a \neq \theta_r$ implies a jump in the value of the contact angle.

A solution to this problem has been suggested by Dussan V. & Chow (1983), who assumed that the drop's CL involves straight-line segments (see figure 8*b*) along which the contact angle changes continuously from θ_a to θ_r, and such segments have indeed been observed experimentally (Bikerman 1950; Furmidge 1962; Rio *et al.* 2005).

An alternative way to introduce a critical inclination angle consists in letting the plate be inhomogeneous. Following this idea, Savva & Kalliadasis (2013) examined 2D drops on an inclined plate with topography and chemical inhomogeneities, and it can be deduced from their results that inhomogeneities can make drops static, for a sufficiently small inclination angle, even if $\theta_a = \theta_r$.

6. Concluding remarks

Thus, we have examined two- and three-dimensional drops sliding down an inclined plate, with their sizes exceeding the slip length l. Our main result is the asymptotic expression (4.32) for the sliding velocity c_* of a three-dimensional thin and small drop (where 'small' means 'with a small Bond number').

The expression for c_* has been matched to a qualitative estimate obtained by Kim *et al.* (2002) for arbitrary drops (not necessarily thin and small). The matching fixes the undetermined coefficient involved in this estimate, transforming it into a *quantitative* result for *arbitrary* drops.

It turns out, however, that the Navier-slip model of CLs (and, hence, our results) agrees with the available experimental data only for an unphysically small slip length.

Still, the dependence on all other parameters does agree with the experiments (under the additional requirement that the drop's Reynolds number be small). Thus, until a physically consistent model of CLs is developed, our results (as well as the underlying Navier-slip model) can still be used in, say, industrial applications.

Generally, given the large number of alternative models of CLs, it would be very interesting to use them to calculate the velocity of sliding drops and compare the results with those of the experiments. This should enable one to determine the model that is not just useful for applications, but is also relevant physically. One such model could be that of Shikhmurzaev (1993), for which Puthenveettil *et al.* (2013) obtained reasonable values for all of the adjustable parameters involved.

Another potential extension of our results consists in introducing a hysteresis interval, i.e. assuming $\theta_a > \theta_r$. If it is sufficiently narrow, and the Bond number is still small, the problem can be treated using an asymptotic approach similar to the one of this work. One can also examine drops on an inhomogeneous substrate: the inhomogeneities (as shown for 2D drops by Savva & Kalliadasis 2013) would produce a similar effect to hysteresis even if $\theta_r = \theta_a$.

Finally, it would be interesting to examine the effect of inertia (by assuming that the drop's Reynolds number is order one). It should be noted, however, that even though it should change the global parameters of the drop, it is unlikely to affect the local dynamics of the CL (due to the extremely small spatial scale of the processes involved).

Acknowledgements

Appendix A. The case of zero contact angle

There seems to exist only one kind of asymptotics of the solution of (2.1) that corresponds to the contact angle being zero. In application to the advancing CL (located at $x = 0$), it has the form

$$h = B(-x)^{3/2} + D(-x)^n + O[(-x)^3] \quad \text{as } x \to -0, \tag{A 1}$$

where B, C and n are undetermined constants. It should be noted that the asymptotics (A 1) is self-consistent only if

$$\tfrac{3}{2} < n < 3. \tag{A 2}$$

On substituting (A 1) into (2.1), we obtain

$$B^2 = \frac{8\mu c_*}{3\sigma l}, \tag{A 3}$$

$$n(n - 1)(n - 2) - \tfrac{3}{8} = 0, \tag{A 4}$$

whereas D remains undetermined (it can be determined by matching the local solution (A 1) to the global one). The cubic (A 4) can be readily solved, and one of its roots,

$$n = \tfrac{1}{4}(5 + \sqrt{13}) \approx 2.15, \tag{A 5}$$

satisfies condition (A 2).

Next, assume asymptotics similar to (A 1), but for the receding CL, i.e.

$$h = B(x + L)^{3/2} + D(x + L)^n + O[(x + L)^3] \quad \text{as } x \to L + 0. \tag{A 6}$$

On substituting this expansion into (2.1), one can verify that n again satisfies (A 4), but

$$B^2 = -\frac{8\mu c_*}{3\sigma l}. \tag{A 7}$$

Thus, no real solutions exist for a receding CL with zero contact angle.

Appendix B. The numerical method for problem (2.6)–(2.8)

When computing the solution of the boundary-value problem (2.6)–(2.8), the main difficulty results from the fact that (2.6) is singular at both boundaries (where the coefficient of the highest derivative vanishes).

To bypass this difficulty, observe that (2.6) admits a Frobenius-style expansion about $x = -L$,

$$\begin{aligned}
h &= P_1(x+L) + P_2(x+L)^2 + Q_2(x+L)^2 \ln(x+L) + P_3(x+L)^3 \\
&\quad + Q_3(x+L)^3 \ln(x+L) + O[(x+L)^4 \ln^2(x+L)] \quad \text{as } x \to -L+0. \tag{B 1}
\end{aligned}$$

On substituting (B 1) into (2.6) and (2.7), one obtains

$$\left.\begin{aligned}
P_1 &= 1, \quad P_3 = -\left(\frac{1}{9\lambda} + \frac{Q_2}{3}\right)\frac{c}{2\lambda} - \frac{11c^2 + 12\lambda^2}{72\lambda^2}, \\
Q_2 &= \frac{c}{2\lambda}, \quad Q_3 = -\frac{c^2}{12\lambda^2}.
\end{aligned}\right\} \tag{B 2}$$

A similar expansion can be derived from (2.6) and the boundary condition (2.8) for the vicinity of $x = 0$,

$$h = C_1 x + C_2 x^2 + D_2 x^2 \ln(-x) + C_3 x^3 + D_3 x^3 \ln(-x) + O[x^4 \ln^2(-x)] \quad \text{as } x \to -0, \tag{B 3}$$

where

$$\left.\begin{aligned}
C_1 &= -1, \quad C_3 = -\left(\frac{1}{9\lambda} + \frac{D_2}{3}\right)\frac{c}{2\lambda} - \frac{11c^2 + 12\lambda^2}{72\lambda^2}, \\
D_2 &= -\frac{c}{2\lambda}, \quad D_3 = \frac{c^2}{12\lambda^2}.
\end{aligned}\right\} \tag{B 4}$$

We observe that the coefficients P_2 and C_2 remain undetermined (they can only be fixed by matching the local expansions (B 1) and (B 3) to the global solution).

Expressions (B 1)–(B 2) and (B 3)–(B 4) can be used to 'shift' the boundary conditions away from the singular points $x = -L$ and $x = 0$ to $x = -L + \Delta$ and $x = -\Delta$ (where Δ is small). Thus, (2.7) and (2.8) are to be replaced with

$$\begin{aligned}
(h)_{x=-L+\Delta} &= \Delta + P_2\Delta^2 + \frac{c}{2\lambda}\Delta^2 \ln \Delta \\
&\quad - \left[\left(\frac{1}{9\lambda} + \frac{Q_2}{3}\right)\frac{c}{2\lambda} + \frac{11c^2 + 12\lambda^2}{72\lambda^2}\right]\Delta^3 - \frac{c^2}{12\lambda^2}\Delta^3 \ln \Delta, \tag{B 5}
\end{aligned}$$

$$\begin{aligned}
\left(\frac{dh}{dx}\right)_{x=-L+\Delta} &= 1 + 2P_2\Delta + \frac{c}{2\lambda}\Delta(2\ln\Delta + 1) \\
&\quad - 3\left[\left(\frac{1}{9\lambda} + \frac{Q_2}{3}\right)\frac{c}{2\lambda} + \frac{11c^2 + 12\lambda^2}{72\lambda^2}\right]\Delta^2 - \frac{c^2}{12\lambda^2}\Delta^2(3\ln\Delta + 1),
\end{aligned}$$
$$\tag{B 6}$$

$$(h)_{x=-\Delta} = -\Delta + C_2 \Delta^2 - \frac{c}{2\lambda} \Delta^2 \ln \Delta$$
$$- \left[\left(\frac{1}{9\lambda} + \frac{D_2}{3} \right) \frac{c}{2\lambda} + \frac{11c^2 + 12\lambda^2}{72\lambda^2} \right] \Delta^3 + \frac{c^2}{12\lambda^2} \Delta^3 \ln(-x), \quad \text{(B 7)}$$

$$\left(\frac{dh}{dx} \right)_{x=-\Delta} = -1 + 2C_2 \Delta - \frac{c}{2\lambda} \Delta (2 \ln \Delta + 1)$$
$$- 3 \left[\left(\frac{1}{9\lambda} + \frac{D_2}{3} \right) \frac{c}{2\lambda} + \frac{11c^2 + 12\lambda^2}{72\lambda^2} \right] \Delta^2 + \frac{c^2}{12\lambda^2} \Delta^2 [3 \ln(-x) + 1]. \tag{B 8}$$

To eliminate the undetermined constant P_2, one needs to differentiate (B 1) twice, evaluate the resulting expression at $x = -L + \Delta$, and compare it with (B 6), which yields

$$P_2 = \frac{2 \left(\dfrac{dh}{dx} \right)_{x=-L+\Delta} - \Delta \left(\dfrac{d^2 h}{dx^2} \right)_{x=-L+\Delta} - 2 - \dfrac{c}{2\lambda} \Delta (2 \ln \Delta - 1) - \dfrac{c^2}{4\lambda^2} \Delta^2}{2\Delta}. \tag{B 9}$$

A similar expression can be derived for C_2:

$$C_2 = \frac{-2 \left(\dfrac{dh}{dx} \right)_{x=-\Delta} - \Delta \left(\dfrac{d^2 h}{dx^2} \right)_{x=-\Delta} - 2 + \dfrac{c}{2\lambda} \Delta (2 \ln \Delta - 1) - \dfrac{c^2}{4\lambda^2} \Delta^2}{2\Delta}. \tag{B 10}$$

Upon substitution of (B 9) and (B 10) into (B 5)–(B 8), the latter become closed-form boundary conditions for h and its derivatives, and these boundary conditions are set at regular points of (2.6).

The boundary-value problem (2.6), (B 5)–(B 8) was solved for $h(x)$ and c using the MATLAB function BVP5C (designed for solving an nth order ordinary differential equation involving m eigenvalues, with $n + m$ boundary conditions). The algorithm employed by BVP5C is based on the four-stage Lobatto IIIa formula (see Ascher, Mattheij & Russell 1995).

The solution found through the above procedure turned out to be virtually independent of Δ as long as $\Delta \leqslant \lambda/10$.

Appendix C. The boundary-value problem (3.43)–(3.45)

C.1. *The asymptotics (3.46)*

It is convenient to rearrange (3.43) using two consecutive changes of variables,

$$(x_e, h_e) \to \left(h_e, p = \frac{dh_e}{dx_e} \right) \to (\eta = -\ln h_e, p), \tag{C 1}$$

after which (3.43) becomes

$$\frac{p}{2} \frac{d^2(p^2)}{d\eta^2} + \frac{1}{3} \frac{d(p^3)}{d\eta} + e^{-2\eta} = 3. \tag{C 2}$$

In terms of the new variables, the asymptotics (3.46) corresponds to the limit

$$p \to \infty \quad \text{as} \quad \eta \to \infty, \tag{C 3}$$

which can be 'targeted' by scaling the variables as follows:

$$\eta = \frac{\eta_{new}}{\epsilon}, \quad p = \frac{p_{new}}{\epsilon^{1/3}}, \tag{C 4a,b}$$

and taking the limit $\epsilon \to 0$. On substituting (C 4) into (C 2) and omitting the subscript *new*, we obtain

$$\frac{\epsilon p}{2} \frac{d^2(p^2)}{d\eta^2} + \frac{1}{3} \frac{d(p^3)}{d\eta} + \exp\left(-\frac{2\eta}{\epsilon}\right) = 3. \tag{C 5}$$

We seek a solution of the form

$$p = \sum_{k=0}^{\infty} \epsilon^k p_k + O\left[\exp\left(-\frac{2\eta}{\epsilon}\right)\right] \quad \text{as } \eta \to \infty, \tag{C 6}$$

where p_0, p_1 and p_2 satisfy

$$\frac{1}{3} \frac{d(p_0^3)}{d\eta} = 3, \tag{C 7}$$

$$\frac{p_0}{2} \frac{d^2(p_0^2)}{d\eta^2} + \frac{1}{3} \frac{d(3p_0^2 p_1)}{d\eta} = 0, \tag{C 8}$$

$$\frac{p_1}{2} \frac{d^2(p_0^2)}{d\eta^2} + \frac{p_0}{2} \frac{d^2(2p_0 p_1)}{d\eta^2} + \frac{1}{3} \frac{d(3p_0^2 p_2 + 3p_0 p_1^2)}{d\eta} = 0. \tag{C 9}$$

The general solutions of these equations are

$$\left.\begin{array}{c} p_0 = [9(\eta + a_0)]^{1/3}, \\[2mm] p_1 = \dfrac{\ln(\eta + a_0) + a_1}{[9(\eta + a_0)]^{2/3}}, \\[3mm] p_2 = -\dfrac{[\ln(\eta + a_0)]^2 - 3\ln(\eta + a_0) + 12}{[9(\eta + a_0)]^{5/3}} + \dfrac{a_2}{[9(\eta + a_0)]^{2/3}}, \end{array}\right\} \tag{C 10}$$

where a_0, a_1 and a_2 are constants of integration. On comparing the expressions for p_1 and p_2, one can see that a_2 can be eliminated by a small ($\sim\epsilon$) change of a_1. Next, we observe that

$$p_0 = (9\eta)^{1/3} + \frac{3a_0}{(9\eta)^{2/3}} + O\left[\frac{1}{(9\eta)^{5/3}}\right], \quad p_1 = \frac{\ln\eta + a_1}{(9\eta)^{2/3}} + O\left[\frac{\ln\eta}{(9\eta)^{5/3}}\right] \quad \text{as } \eta \to \infty, \tag{C 11a,b}$$

which means that, in the limit $\eta \to \infty$, a_0 can also be eliminated by changing a_1. Setting, thus,

$$a_0 = a_2 = 0, \tag{C 12}$$

we substitute (C 10)–(C 13) into (C 6):

$$p = (9\eta)^{1/3} + \frac{\epsilon(\ln\eta + a_1)}{(9\eta)^{2/3}} - \frac{\epsilon^2(\ln^2\eta - 3\ln\eta + 12)}{(9\eta)^{5/3}} + O\left[\frac{\ln^3\eta}{(9\eta)^{8/3}}\right]. \tag{C 13}$$

The parameter ϵ has played its role of the 'indicator' of small terms and can now be omitted. Setting accordingly $\epsilon = 1$, we rewrite (C 13) in terms of the original

variables,

$$
\begin{aligned}
\frac{\mathrm{d}h_e}{\mathrm{d}x_e} = {} & -(9\ln h_e)^{1/3} + \frac{\ln(-\ln h_e) + a_1}{(9\ln h_e)^{2/3}} \\
& + \frac{\ln^2(-\ln h_e) - 3\ln(-\ln h_e) + 12}{(9\ln h_e)^{5/3}} + O\left[\frac{\ln^3(-\ln h_e)}{\ln^{8/3} h_e}\right].
\end{aligned} \tag{C 14}
$$

Equation (C 14) should be treated as a first-order ordinary differential equation for $h_e(x_e)$. Seeking a solution in a form similar to that of the right-hand side of (C 14), one can derive the desired asymptotics (3.46) and also obtain

$$
b = -3 + 2\ln 3 - a_1. \tag{C 15}
$$

C.2. *Numerical solution of problem (3.43)–(3.45)*

The simplest numerical approach to solving the boundary-value problem (3.43)–(3.45) consists in 'shooting' the solution from a large positive value of x_e (approximating plus-infinity) towards $x_e = 0$.

The boundary condition (3.44) suggests that, for large x_e,

$$
h_e \sim 3^{1/2} + \hat{h}, \tag{C 16}
$$

where

$$
\hat{h} \to 0 \quad \text{as } x_e \to \infty. \tag{C 17}
$$

By linearising (3.43) with respect to $\hat{h}$, solving the resulting equation subject to the boundary condition (C 17) and substituting $\hat{h}$ into (C 16), we obtain

$$
h_e \sim 3^{1/2} + C\exp\left(-\frac{2}{3^{1/2}}x_e\right) \quad \text{as } x_e \to \infty, \tag{C 18}
$$

where C is an arbitrary constant. It turns out that, if $C > 0$, the solution h_e is positive for all x_e and the boundary condition (3.46) cannot be satisfied; hence, C must be negative. Its absolute value, however, is unimportant, as changing it amounts to shifting the solution along the x_e-axis without changing its shape. Thus, we can set

$$
C = -1. \tag{C 19}
$$

It turns out that the solution determined by the asymptotics (C 18) and (C 19) vanishes at $x_e = \hat{x}_e \approx -0.2610$, not at $x_e = 0$; hence, the boundary condition (3.45) does not hold. This can be corrected by shifting the x_e-axis by $\hat{x}_e$.

The above algorithm was realised using MATLAB's function ODE45 based on an explicit Runge–Kutta (4,5) formula, the Dormand–Prince pair (Dormand & Prince 1980). Since (3.43) becomes singular at the point where h_e vanishes, the computation was stopped when h_e became smaller than 10^{-12}. This was achieved through the 'Event' option of ODE45, which would stop the computation once an appropriately chosen 'event function' changed its sign.

C.3. *Computation of the constant b*

It appears that b can be computed by shooting two solutions from $x_e = 0$ and $x_e = +\infty$, using the asymptotics (3.46) and (C 18) respectively, and matching them at an intermediate point by adjusting the constants b and C. However, matching the two solutions implies continuity of h_e, $\mathrm{d}h_e/\mathrm{d}x$ and $\mathrm{d}^2 h_e/\mathrm{d}x^2$, which cannot be achieved by adjusting two constants. In principle, it is possible to generalise the asymptotics (3.46) so that it would include an extra constant, but the correction involving this constant becomes exponentially smaller than the rest of the solution as $x_e \to 0$. As a result, if the extra constant is used for shooting, the numerical solution exhibits exponentially strong dependence on the initial conditions, and the iterations do not converge.

Alternatively, b can be found by computing a_1 (which appears in the asymptotics (C 14)) and using expression (C 15) to determine b.

To extract a_1 from the solution $h_e(x_e)$ (computed as described in the previous subappendix), we 'constructed' the following function:

$$f(x_e) = \frac{\mathrm{d}h_e}{\mathrm{d}x_e}(9 \ln h_e)^{2/3} + 9 \ln h_e - \ln(-\ln h_e) - \frac{\ln^2(-\ln h_e) - 3 \ln(-\ln h_e) + 12}{9 \ln h_e}. \quad \text{(C 20)}$$

Comparing this expression with the asymptotics (C 14), one can see that

$$\lim_{h_e \to 0} f = a_1. \quad \text{(C 21)}$$

This approach yields $a_1 \approx -0.189$, for which (C 15) yields $b \approx -0.613$.

REFERENCES

ASCHER, U. M., MATTHEIJ, R. M. M. & RUSSELL, R. D. 1995 *Numerical Solution of Boundary Value Problems for Ordinary Differential Equations*, Classics in Applied Mathematics, vol. 13. SIAM.

BENILOV, E. S., BENILOV, M. S. & KOPTEVA, N. 2008 Steady rimming flows with surface tension. *J. Fluid Mech.* **597**, 81–118.

BENILOV, E. S., CHAPMAN, S. J., MCLEOD, J. B., OCKENDON, J. R. & ZUBKOV, V. S. 2010 On liquid films on an inclined plate. *J. Fluid Mech.* **663**, 53–69.

BERTOZZI, A. L. & BRENNER, M. P. 1997 Linear stability and transient growth in driven contact lines. *Phys. Fluids* **9**, 530–539.

BIKERMAN, J. J. 1950 Sliding of drops from surfaces of different roughnesses. *J. Colloid Sci.* **5**, 349–359.

BOWLES, R. I. 1995 Upstream influence and the form of standing hydraulic jumps in liquid-layer flows on favourable slopes. *J. Fluid Mech.* **284**, 63–96.

COX, R. G. 1986 The dynamics of the spreading of liquids on a solid surface. Part 1. Viscous flow. *J. Fluid Mech.* **168**, 169–194.

DORMAND, J. R. & PRINCE, P. J. 1980 A family of embedded Runge–Kutta formulae. *J. Comput. Appl. Maths* **6**, 19–26.

DUCHEMIN, L., LISTER, J. R. & LANGE, U. 2005 Static shapes of levitated viscous drops. *J. Fluid Mech.* **533**, 161–170.

DUSSAN V., E. B. & CHOW, R. T.-P. 1983 On the ability of drops or bubbles to stick to non-horizontal surfaces of solids. *J. Fluid Mech.* **137**, 1–29.

FURMIDGE, C. G. L. 1962 Studies at phase interfaces. I. The sliding of liquid drops on solid surfaces and a theory for spray retention. *J. Colloid Sci.* **17**, 309–324.

GLASSMAKER, N. J., JAGOTA, A., HUI, C. Y., NODERER, W. L. & CHAUDHURY, M. K. 2007 Biologically inspired crack trapping for enhanced adhesion. *Proc. Natl Acad. Sci. USA* **104**, 10786–10791.

HOCKING, L. M. 1981 Sliding and spreading of thin two-dimensional drops. *J. Mech. Appl. Maths* **34**, 37–55.

HOCKING, L. M. & RIVERS, A. D. 1982 The spreading of a drop by capillary action. *J. Fluid Mech.* **121**, 425–442.

HUPPERT, H. 1982 Flow and instability of a viscous current down a slope. *Nature* **300**, 427–439.

JERRETT, J. M. & DE BRUYN, J. R. 1992 Finger instability of a gravitationally driven contact line. *Phys. Fluids* A **4**, 234–242.

KIM, H.-Y., LEE, H. J. & KANG, B. H. 2002 Sliding of liquid drops down an inclined solid surface. *J. Colloid Interface Sci.* **247**, 372–380.

KOH, Y. Y., LEE, Y. C., GASKELL, P. H., JIMACK, P. K. & THOMPSON, H. M. 2009 Droplet migration: quantitative comparisons with experiment. *Eur. Phys. J. Spec. Top.* **166**, 117–120.

LACEY, A. A. 1982 The motion with slip of a thin viscous droplet over a solid-surface. *Stud. Appl. Maths* **67**, 217–230.

LE GRAND, N., DAERR, A. & LIMAT, L. 2005 Shape and motion of drops sliding down an inclined plane. *J. Fluid Mech.* **541**, 293–315.

LIMAT, L. 2014 Drops sliding down an incline at large contact line velocity: what happens on the road towards rolling? *J. Fluid Mech.* **738**, 1–4.

PODGORSKI, T., FLESSELLES, J.-M. & LIMAT, L. 2001 Corners, cusps, and pearls in running drops. *Phys. Rev. Lett.* **87**, 036102,1–4.

PUTHENVEETTIL, B. A., SENTHILKUMAR, V. K. & HOPFINGER, E. J. 2013 Motion of drops on inclined surfaces in the inertial regime. *J. Fluid Mech.* **726**, 26–61.

RIO, E., DAERR, A., ANDREOTTI, B. & LIMAT, L. 2005 Boundary conditions in the vicinity of a dynamic contact line: experimental investigation of viscous drops sliding down an inclined plane. *Phys. Rev. Lett.* **94**, 024503,1–4.

SAVVA, N. & KALLIADASIS, S. 2013 Droplet motion on inclined heterogeneous substrates. *J. Fluid Mech.* **725**, 462–491.

SCHWARTZ, L. W., ROUX, D. & COOPER-WHITE, J. J. 2005 On the shapes of droplets that are sliding on a vertical wall. *Physica* D **209**, 236–244.

SHIKHMURZAEV, Y. U. D. 1993 The moving contact line on a smooth solid surface. *Intl J. Multiphase Flow* **19**, 589–610.

SIBLEY, D. N., NOLD, A. & KALLIADASIS, S. 2015 The asymptotics of the moving contact line: cracking an old nut. *J. Fluid Mech.* **764**, 445–462.

SILVI, N. & DUSSAN V., E. B. 1985 On the rewetting of an inclined solid surface by a liquid. *Phys. Fluids* **28**, 5–7.

SMITH, J. D., DHIMAN, R., ANAND, S., REZA-GARDUNO, E., COHEN, R. E., McKINLEYA, G. H. & VARANASI, K. K. 2013 Droplet mobility on lubricant-impregnated surfaces. *Soft Matt.* **9**, 1772–1780.

SNOEIJER, J. H., LE GRAND-PITEIRA, N., LIMAT, L., STONE, H. A. & EGGERS, J. 2007 Cornered drops and rivulets. *Phys. Fluids* **19**, 042104,1–10.

THIELE, U. & KNOBLOCH, E. 2003 Front and back instability of a liquid film on a slightly inclined plate. *Phys. Fluids* A **15**, 892–907.

THIELE, U., NEUFFER, K., BESTEHORN, M., POMEAU, Y. & VELARDE, M. G. 2002 Sliding drops on an inclined plane. *Collids Surf.* A **206**, 87–104.

VOINOV, O. V. 1976 Hydrodynamics of wetting. *Fluid Dyn.* **11**, 714–721.

WILSON, S. D. R. & JONES, A. F. 1983 The entry of a falling film into a pool and the air-entrainment problem. *J. Fluid Mech.* **128**, 219–230.

WINKELS, K. G., PETERS, I. R., EVANGELISTA, F., RIEPEN, M., DAERR, A., LIMAT, L. & SNOEIJER, J. H. 2011 Receding contact lines: from sliding drops to immersion lithography. *Eur. Phys. J. Spec. Top.* **192**, 195–205.